Polymorphism and "reverse" spin transition in the spin crossover system $[Co(4\text{-terpyridone})_2](CF_3SO_3)_2\cdot 1H_2O$†

Gloria Agustí,[a] Carlos Bartual,[a] Víctor Martínez,[a] Francisco J. Muñoz-Lara,[a] Ana B. Gaspar,[a] M. Carmen Muñoz[b] and José A. Real*[a]

Received (in Montpellier, France) 20th March 2009, Accepted 31st March 2009
First published as an Advance Article on the web 23rd April 2009
DOI: 10.1039/b905674b

Compound $[Co(4\text{-terpyridone})_2](CF_3SO_3)_2\cdot 1H_2O$, where 4-terpyridone is 2,6-bis(2-pyridyl)-4(1*H*)-pyridone, forms two polymorphs. Polymorph **1** displays a continuous spin conversion in the temperature region 300–120 K while polymorph **2** shows, on cooling, the onset of a continuous high-spin (HS) to low-spin (LS) conversion interrupted by an abrupt "reverse" spin transition in the temperature region 217–203 K. The formed unstable HS intermediate phase (IP) undergoes a strong cooperative "normal" spin transition characterised by a hysteresis loop 33 K wide. The structural data give support for a crystallographic phase transition, which takes place concomitantly with the "reverse" spin state transition.

Introduction

Spin crossover (SCO) materials display labile electronic configurations switchable between the high-spin (HS) and low-spin (LS) states leading to distinctive changes in magnetism, colour and structure, which may be driven by a variation of temperature and/or pressure and by light irradiation.[1] In the solid state, their magnetic, optical and structural properties may be changed drastically in a narrow range of temperature and/or pressure for cooperative spin transitions. In some cases, the transition displays a hysteretic behaviour (memory effect) conferring to the material a bistable character.[2–4]

Most SCO compounds investigated so far involve Fe(II) and Fe(III) complexes and to a lesser extent Co(II).[5] The Co(II) ion experiences a change between the $^2E(t_{2g}^6eg^1)$ ($S = 1/2$) and $^4T_1(t_{2g}^5eg^2)$ ($S = 3/2$) ground states involving the transfer of just one electron. This is the cause of the significant structural, thermodynamic and kinetic differences observed in the Co(II) SCO behaviour with respect to Fe(II) complexes.[6] The relevant structural parameter, the Co–N bond distances, changes approximately by 0.10 Å on average. Hence, the volume change associated with the SCO in a Co(II) complex is approximately 50% less than for an Fe(II) complex. This can explain the observed continuous nature of the SCO for the vast majority of Co(II) complexes.

Discrete mono-,[7–16] di-[17,18] and trinuclear[19–21] species as well as 1D[22] polymeric Co(II) SCO complexes have been reported so far. $[Co(terpy)_2]X_p\cdot nH_2O$ (terpy = 2,2′:6′,2″-terpyridine; X = halide, pseudohalide, NO_3^-, ClO_4^-)[7,8] and $[Co(H_2\text{-}fsa_2en)L_2]$ (H_2-fsa_2en = *N*,*N*′-*o*-ethylene-bis-(3-carboxy-salicylaldiiminate); L = pyridine, substituted pyridines and H_2O) have been intensively studied.[9–12] The latter series of compounds exhibit the most abrupt transitions ever observed for Co(II) complexes while the former series display rather continuous SCO behaviour. More recently, a series of $[Co(4\text{-terpyridone})_2]X_p\cdot nS$ complex salts where 4-terpyridone is 2,6-bis(2-pyridyl)-4(1*H*)-pyridone, X = halide, NO_3^-, ClO_4^-, BF_4^-, PF_6^-, BF_4^-/SiF_6^{2-}, SO_4^{2-} and $[Co(NCS)_4]^{2-}$and S = H_2O and/or MeOH were synthesised and the influence of the anion on the SCO behaviour was discussed.[23,24]

The presence of the reactive ketone group in the 4-terpyridone ligand has facilitated the attachment of long alkyl chains bonded to the oxygen in the 4-position of the central pyridine ring. The aim was to discover synergies in new bifunctional materials able to display both liquid crystal and SCO properties. This has enabled to produce a series of $[Co(4\text{-terpyOR})_2]X_p\cdot nS$ complexes.[25] In particular, the complex $[Co(4\text{-terpyOC}_{16})_2](BF_4)_2\cdot n$MeOH (4-terpyOC$_{16}$ = 4′-hexadecyloxy-2,2′:6′,2″-terpyridine) displays a very continuous SCO when $n = 1$ but, unexpectedly, the non-solvated form undergoes an abrupt "reverse" spin transition (from LS to HS state on lowering temperature and from HS to LS state on warming). This singular spin transition, triggered by a concomitant crystallographic phase transition, was associated with the change in the crystal packing of the long alkyl chains resulting in the stabilisation of the HS state for the Co(II) cations.[25a]

Reverse spin state transition has been observed as well in the SCO metallomesogens $[Fe(C_n\text{-tameMe})](BF_4)_2$ (n = 10, 12, 14, 16, 17, 18; C_n-tameMe = 2,2,2-tris(2-aza-3-((5-alkoxy)-(6-methyl)(2-pyridyl))prop-2-enyl)ethane). These Fe(II) metallomesogens show thermally driven spin crossover and mesomorphism above 300 K. All experimental data point out that the structural rearrangement of the metallomesogens upon crystal ↔ smectic transition is the origin of a partial "reverse" spin transition observed in the course of the thermally driven SCO.[25d]

[a] *Institut de Ciència Molecular (ICMol)/Departament de Química Inorgànica, Universitat de València, Edifici de Instituts de Paterna, P. O. Box 22085, 46071, València, Spain. E-mail: jose.a.real@uv.es*
[b] *Departament de Física Aplicada, Universitat Politècnica de València, Camí de Vera s/n, 46022, València, Spain*

† Electronic supplementary information (ESI) available: Table S1: Crystal data and selected bond lengths and angles for **1** at 120 K. Table S2: Crystal data for **2** at 180 K and 120 K. CCDC reference numbers 725083–725085. For ESI and crystallographic data in CIF or other electronic format see DOI: 10.1039/b905674b

Here we report the synthesis, structure and magnetic properties of two polymorphs of the new salt $[Co(4\text{-terpyridone})_2](CF_3SO_3)_2 \cdot 1H_2O$. Polymorph **1** undergoes a continuous spin transition while polymorph **2** displays a singular "reverse" spin transition followed by a strong cooperative spin transition characterised by a hysteresis loop 33 K wide.

Results

Magnetic properties

The magnetic behaviour of compounds **1** and **2** in the form of the product $\chi_M T$ *vs.* T, where χ_M is the molar magnetic susceptibility and T temperature, is shown in Fig. 1. At 300 K, $\chi_M T$ is 2.41 and 2.70 cm^3 K mol^{-1} for **1** and **2**, respectively. These values correspond well with the expected one for a cobalt(II) ion in the $S = 3/2$ HS state with an important orbital contribution. For **1**, $\chi_M T$ decreases continuously as T is decreased down to *ca.* 75 K where it takes a value of *ca.* 0.48 cm^3 K mol^{-1}, which is consistent with the $S = 1/2$ LS state of cobalt(II). This behaviour corresponds to a continuous spin transition between the $S = 1/2$ and $S = 3/2$ spin states. For **2**, $\chi_M T$ first decreases continuously between 300 K and 217 K to attain a value of 2.12 cm^3 K mol^{-1}. Then, it increases rapidly up to 2.40 cm^3 K mol^{-1} as T decreases down to 203 K. Upon cooling, $\chi_M T$ decreases moderately between 203 K and 165 K, defining an inclined plateau. Just below this temperature there is a sharp decrease of $\chi_M T$ ($T_c^{\downarrow} = 155.6$ K) to reach similar values to **1** down to 150 K. In the warming mode, this discontinuous behaviour takes place at $T_c^{\uparrow} = 188.5$ K denoting the occurrence of a hysteresis loop 32.9 K wide. $\chi_M T$ increases up to 2.60 cm^3 K mol^{-1} at *ca.* 212 K, a value significantly larger than that observed in the cooling mode; however, in this mode no inclined plateau is observed, and $\chi_M T$ decreases rapidly on warming to join the cooling-mode curve at 225.6 K defining a small hysteresis loop 10–12 K wide.

Crystal structure

The crystal structure of polymorphs **1** and **2** has been investigated at 293 and 120 K;† in addition, we have also measured

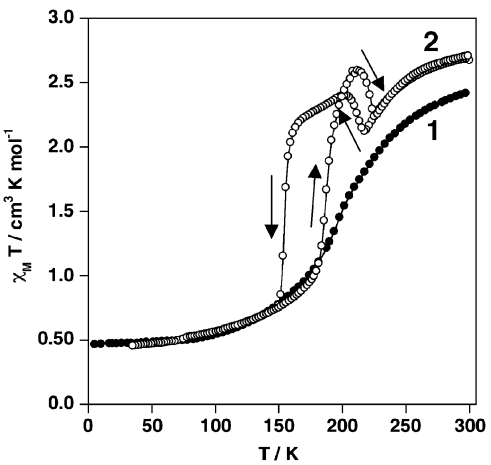

Fig. 1 $\chi_M T$ *vs.* T plot for polymorphs **1** (filled circles) and **2** (open circles). Arrows indicate cooling and warming modes.

Table 1 Crystal data for **1** and **2**

	1 293 K	**2** 293 K
Empirical formula	$C_{32}H_{24}N_6O_9S_2F_6Co$	
M_r	873.62	
Crystal system	Triclinic	
Space group	$P\bar{1}$	
a/Å	9.1020(5)	9.5700(4)
b/Å	9.2410(5)	14.3510(9)
c/Å	21.3860(18)	14.9540(8)
α/°	94.896(2)	75.456(4)
β/°	94.487(2)	71.982(4)
γ/°	90.730(6)	72.274(2)
V/Å^3	1786.4(2)	1832.19(17)
Z	2	
D_c/mg cm^{-3}	1.624	1.584
$F(000)$	886	
μ (Mo-K$_\alpha$)/mm^{-1}	0.691	0.674
Crystal size/mm	0.06 × 0.06 × 0.02	0.02 × 0.01 × 0.01
No. of independent reflections	2703	4930
No. of reflections $[I > 2\sigma(I)]$	1854	3365
R_1 $[I > 2\sigma(I)]$	0.0936	0.0903
wR $[I > 2\sigma(I)]$	0.2761	0.2661
S	1.251	1.263

$R_1 = \Sigma\ ||F_o| - |F_c||/\Sigma|F_o|$ w$R = [\Sigma\ [w(F_o^2 - F_c^2)^2]/\Sigma\ [w(F_o^2)^2]]^{1/2}$. $w = 1/[\sigma^2(F_o^2) + (mP)^2 + nP]$ where $P = (F_o^2 + 2F_c^2)/3$. $m = 0.2000$ (**1**), and 0.2000 (**2**); $n = 0.0000$ (**1**), and 0.0000 (**2**).

polymorph **2** at 180 K just in the middle of the inclined plateau formed in the cooling mode just after the jump of $\chi_M T$ *vs.* T curve. Unfortunately, the triflate anions are strongly disordered, a fact that, together with the quality of the crystals, prevented us from getting good crystal data, particularly at low temperatures.

At 293 K, crystals of both polymorphs display the same triclinic $P\bar{1}$ space group but their crystal parameters are significantly different (see Table 1). A selection of bond distances and angles as well as short intermolecular interactions are shown in Table 2. Both polymorphs are constituted of discrete cationic complexes $[Co(4\text{-terpyridone})_2]^{2+}$, two triflate anions and one molecule of water. Fig. 2 displays the structure of the cation together with the corresponding atom numbering. The tridentate 4-terpyridone ligands coordinate the cobalt(II) ion in a *mer* fashion defining a tetragonally compressed $[CoN_6]$ distorted octahedron. The 4-terpyridone ligands adopt the enol form after coordination. The Co–$N_{central}$ axial bonds, Co–N(2) = 1.991(13) [2.018(8)] Å and Co–N(5) = 2.005(15) [2.011(6)] Å for **1** and [**2**], involving the 4-pyridinol moieties are markedly shorter than the equatorial Co–N_{distal} bonds, Co–N(1) = 2.151(13) [2.151(7)] Å, Co–N(3) = 2.146(14) [2.118(8)] Å, Co–N(4) = 2.120(14) [2.148(7)] Å and Co–N(6) = 2.165(14) [2.151(7)] Å.

The average Co–N bond distance of the $[CoN_6]$ core is virtually the same for **1** (2.096(14) Å) and **2** (2.099(7) Å). The major difference was found for the Co–$N_{central}$ bond, which is 0.016 Å larger for **2**. These values are consistent with those previously reported for the $[Co(4\text{-terpyridone})_2]^{2+}$ cation in the HS state. Due to steric restrictions imposed by the ligands the N(1)–Co–N(2), N(2)–Co–N(3), N(4)–Co–N(5) and N(5)–Co–N(6) angles were found to be in the range 78–76° while the N(1)–Co–N(5), N(2)–Co–N(4), N(2)–Co–N(6) and

Table 2 Selected bond lengths [Å] and angles [°] for **1** and **2**

	1 293 K	**2** 293 K
Co(1)–N(1)	2.151(13)	2.151(7)
Co(1)–N(2)	1.991(13)	2.018(8)
Co(1)–N(3)	2.146(14)	2.118(8)
Co(1)–N(4)	2.120(14)	2.148(7)
Co(1)–N(5)	2.005(15)	2.011(6)
Co(1)–N(6)	2.165(14)	2.151(7)
N(1)–Co–N(2)	77.6(7)	76.2(3)
N(1)–Co–N(3)	155.3(7)	153.0(3)
N(1)–Co–N(4)	93.6(5)	93.7(3)
N(1)–Co–N(5)	102.2(6)	99.8(3)
N(1)–Co–N(6)	90.6(5)	92.4(3)
N(2)–Co–N(3)	77.8(7)	76.9(3)
N(2)–Co–N(4)	104.4(6)	102.3(3)
N(2)–Co–N(5)	177.5(6)	175.9(3)
N(2)–Co–N(6)	101.5(6)	104.4(3)
N(3)–Co–N(4)	93.9(5)	93.9(3)
N(3)–Co–N(5)	102.3(6)	107.1(3)
N(3)–Co–N(6)	92.9(5)	92.3(3)
N(4)–Co–N(5)	78.1(7)	77.0(3)
N(4)–Co–N(6)	154.0(7)	153.4(3)
N(5)–Co–N(6)	76.0(7)	76.4(3)

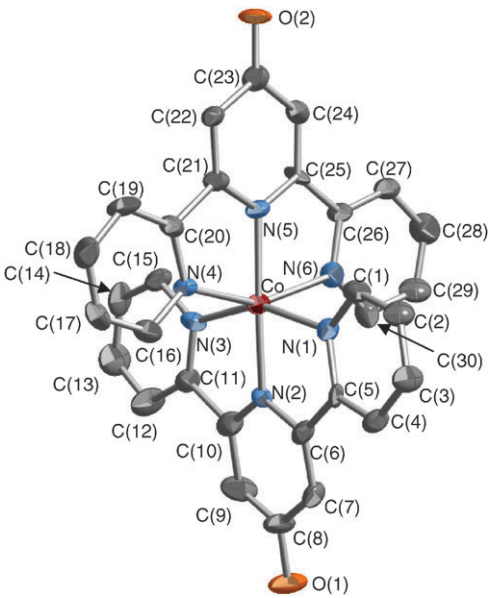

Fig. 2 ORTEP representation of the complex cation. Thermal ellipsoids are presented at 30% of probability.

N(3)–Co–N(5) angles are in the range 100°–107°. Both series of angles are quite far from 90°, the expected value for an ideal octahedron. As a consequence, the N(1)–Co–N(3) and N(4)–Co–N(6) angles separate markedly, *ca.* 25°, from 180° corroborating the distorted nature of the [CoN_6] core.

There are two crystallographically distinct [O_3S–CF_3]$^-$ triflate anions, which display an alternate conformation when projected along the S–C bond. The triflate (T1) defined by the sulfur atom S(1) is only slightly distorted; in contrast, the triflate (T2) defined by the atom S(2) appears strongly distorted due to disorder. This disorder is stronger at low temperatures and prevents a good determination of the crystal structure in the LS state ($R \approx 15\%$). A rough estimate of the average Co–N bond distance at 120 K gives a value of

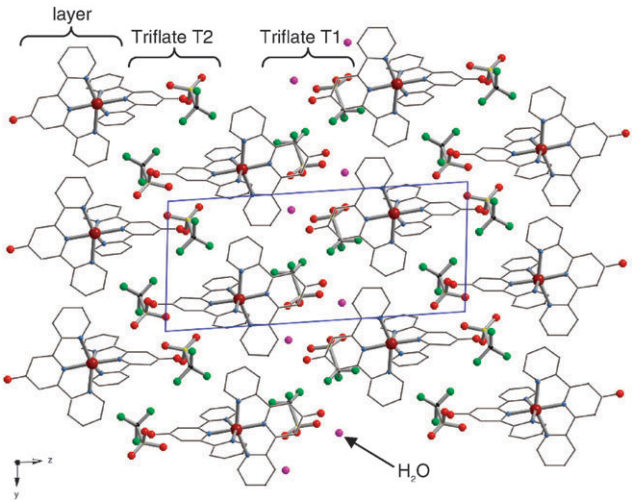

Fig. 3 Projection of the crystal packing of polymorph **1** on the *yz* plane.

2.030(12) Å for **1**, which corresponds to a bond length variation *ca.* 0.07 Å, a value close to the maximum estimated for a $S = 3/2$–$S = 1/2$ (0.1 Å) spin transition (see Table S1, ESI†).

Fig. 3 shows the crystal packing of **1** seen along the [100] direction. It can be described as constituted of layers of complex cations lying in the *xy* plane where short C···C contacts (smaller than the sum of the van der Waals radii, 3.70 Å) indicate the occurrence of π–π stacking: *d*[C(15)···C(2)^{i}] = 3.60(3) Å, *d*[C(14)···C(2)^{i}] = 3.55(3) Å, d[C(14)···C(1)^{i}] = 3.64(3) Å and *d*[C(13)···C (4)^{i}] = 3.58(3) Å (i = $x + 1$, y, z) along the *x* direction and *d*[C(17)···C(28)^{ii}] = 3.66(3) Å, *d*[C(17)···C(27)^{ii}] = 3.57(3) Å, d[C(18)···C(27)^{ii}] = 3.66(3) Å and *d*[C(16)···C(28)^{ii}] = 3.55(3) Å (ii = x, $y - 1$, z) along the *y* direction (see Fig. 4a). An infinite stack of equivalent layers running along the *z* direction conforms the crystal packing.

The inter-planar space is filled alternately by the T1 and T2 triflate anions. Strong discrete hydrogen bonds are formed between the T1 anion (O(6) and O(5)), the O(2) atom belonging to one 4-pyridinol moiety and the water molecule (O(3)) located in the same inter-planar space *d*[O(3)···O(2)^{iii}] = 2.60(2) Å (iii = x, y, $z + 1$), *d*[O(3)···O(5)^{iv}] = 2.80(2) Å (iv = $-x + 1$, $-y$, $-z + 1$) and *d*[O(3)···O(6)] = 2.81(2) Å. These interactions assemble two cations, two anions and two molecules of water (see Fig. 4b). In the adjacent inter-planar spaces the F(5) atom of the T2 triflate forms a strong hydrogen bond with the O(1) of the 4-pyridinol moiety of the other 4-terpyridone ligand.

In compound **2** the cations organise in similar layers as described for **1** but now the layers are oriented in the [1,−1,−1] direction. The number of C···C contacts is smaller than in **1**, *d*[C(16)···C(18)^{i}] = 3.49(2) Å, *d*[C(17)···C(18)^{i}] = 3.56(2) Å, *d*[C(17)···C(17)^{i}] = 3.55(2) Å (i = $-x$, $-y-1$, $-z$), *d*[C(15)···C (3)^{ii}] = 3.69(2) Å and *d*[C(14)···C(4)^{ii}] = 3.61(2) Å (ii = $x + 1$, y, z). As in **1**, the space between the layers is filled with two crystallographically distinct triflate anions and one molecule of water, but unlike **1** all inter-planar spaces are filled identically (Fig. 5a). There are noticeable discrete hydrogen bond interactions: *d*[O(1)···O(3)^{iii}] = 2.65(2) Å

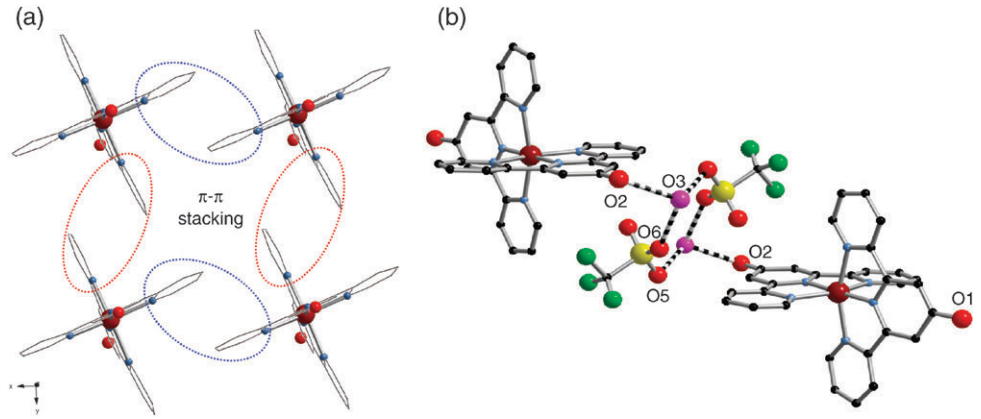

Fig. 4 (a) Packing of the cations within the layers (projection in the *xy* plane) showing the π–π overlapping between the 4-terpyridone ligands for polymorph **1**. (b) Assembly of pairs of complex cations, triflate anions and water molecules *via* hydrogen bonds (broken rods) for polymorph **1**.

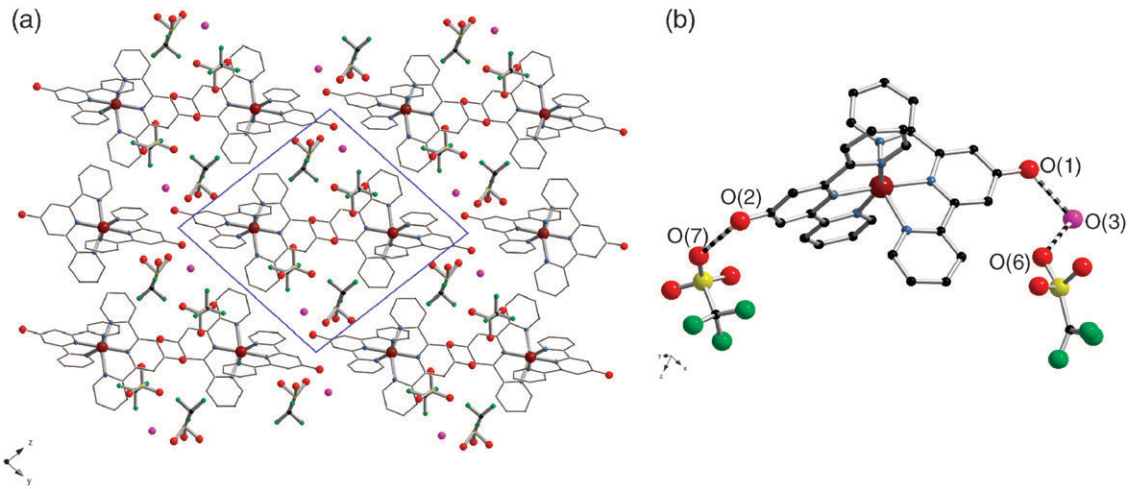

Fig. 5 (a) Crystal packing of polymorph **2**. (b) Interaction *via* hydrogen bonds of the complex cation, the anions and the water molecule in **2**.

(iii = $x - 1$, y, $z - 1$), d[O(3)···O(6)] = 2.89(5) Å and d[O(2)···O(7)] = 2.675(10) Å (Fig. 5b).

As stated above, the same crystal of polymorph **2** was measured in the cooling mode at 180 K, 120 K and again at 293 K. Besides, the thermal dependence of the crystal cell parameters was measured over several cycles in an independent experiment confirming the reversibility of the phenomenon. As for **1**, the disorder of the triflate anions is a major problem in order to solve accurately the structure of **2** at low temperatures. However, a few conclusions can be drawn from these experiments. At 180 K the crystal is at the middle of the inclined plateau defined by the $\chi_M T$ *vs.* T plot just after the LS-to-HS "reverse" in the cooling mode (Fig. 1). At this temperature the a parameter, 18.6610(6) Å, is almost double than that measured at 293 K; consequently, the volume of the unit cell changes from 1786.4(2) $Å^3$ (293 K) to 3539.9(2) $Å^3$ (see Table S2, ESI†). In this intermediate phase (IP), the packing is essentially the same as at 293 K but there are two crystallographically distinct $[Co(4\text{-terpyridone})_2]^{2+}$ cations which segregate along the [001] direction defining alternate layers of Co(1)–Co(2) sites lying in the *xy* plane. Consequently, there are four $[CF_3SO_3]^-$ anions and two molecules of water crystallographically different. The average Co–N bonds in the Co(1) and Co(2) sites are virtually identical to each other (2.024(10) and 2.027(10) Å, respectively) and *ca.* 0.074 Å shorter than at 293 K. This value is consistent with the variation of the average bond lengths upon spin conversion estimated for **1**; however, in the case of **2** the magnetic behaviour indicates that the complex remains in the HS state.

Discussion

Polymorphic materials are those in which the constituent molecules can crystallise in two or more structures. Polymorphism is an issue of great interest for fundamental and practical reasons.[26] From a fundamental viewpoint the study of polymorphism enables an understanding of the mechanisms that control the genesis and properties of such crystalline materials. This is particularly meaningful in the realm of the SCO phenomenon as the constitutive switchable molecules are strongly sensitive to subtle structural modifications. This fact was recognised from the very first studies of the SCO phenomenon and it is particularly well documented for iron(II) complexes (see ref. 4 and references therein).

As far as we know, $[Co(4\text{-terpyridone})_2](BF_4)_2{\cdot}H_2O$ was the first reported example of polymorphism in a cobalt(II) SCO

system, which has been structurally characterised. The packing of the complex cations is quite similar for the BF_4^- and $CF_3SO_3^-$ derivatives. The BF_4^- salts display two different arrangements for the hydrogen bond interactions: in polymorph **1** pairs of BF_4^- anions, water molecules and complex cations are held together *via* strong hydrogen bonds to form discrete units while in polymorph **2** these interactions extend in one dimension. Interestingly, polymorph **1** transforms irreversibly into polymorph **2** in the solid state at temperatures around 325 K. This transformation takes place together with a crystallographic phase transition from the triclinic $P\bar{1}$ space group to the monoclinic $P2_1$ space group. In the $CF_3SO_3^-$ polymorph **1** the hydrogen bond interactions are similar to those described for its BF_4^- counterpart; in contrast, no pair interactions are formed in polymorph **2**. The OH group of the pyridinol moiety of one ligand interacts *via* hydrogen bond with a water molecule, which interacts with an oxygen atom of a $CF_3SO_3^-$ anion. The remaining pyridinol moiety of the complex cation interacts directly *via* hydrogen bond with the oxygen atom of another $CF_3SO_3^-$ anion. In this respect, a similar situation is observed for polymorph **1** but this direct interaction involves a fluorine atom instead of an oxygen atom.

Concerning synthetic aspects, it is well known that to obtain a desired polymorph is not an obvious task to accomplish in molecule-based materials since free energy differences between polymorphs are usually quite small (a few kilojoules per mol) and depend on the entropic contribution to the free energy.[27] This is particularly true when different polymorphs may be compatible within a very small range of temperature; in such cases, kinetic factors influencing nucleation may be crucial for obtaining one of them preferentially. This may be the case of $CF_3SO_3^-$ polymorph **1**; its synthesis is more reliable appearing as large rectangles after slow evaporation of the solvent indicating larger thermodynamic stability; in contrast, polymorph **2** appears as needles preferentially when evaporation is carried out very fast. However, both polymorphs may appear simultaneously in the same preparation.

In the range of temperatures where both BF_4^- polymorphs undergo the SCO behaviour (350–100 K) the $\chi_M T$ values are quite different showing a shift of the characteristic temperatures $T_{1/2}$ of *ca.* 120 K. The irreversible transformation of polymorph **1** into **2** occurs rapidly in a narrow range of temperatures (320 K $< T <$ 340 K). In contrast, no transformation between the $CF_3SO_3^-$ polymorphs has been observed and, further, they change spin state at very similar temperatures. The main difference between the $CF_3SO_3^-$ polymorphs is that the normal continuous pace of the spin state transformation in polymorph **2** is interrupted by the occurrence of a reversible structural phase transition in the temperature range 217–203 K stabilising the HS state in the IP region. Hence, the HS state population increases in the cooling mode reflecting a singular magnetic behaviour reminiscent of the "reverse" spin transition reported by Hayami and co-workers for $[Co(4\text{-terpyOC}_n)_2](BF_4)_2$ (n = 14, 16).[25a] The main difference was found to be the extent of the "reverse" spin transition, which is much less pronounced in the present case since only around 13% of cations reverse their spin state. Despite being limited in magnitude, the reversible structural conversion has a dramatic effect on the nature of the subsequent "normal" spin transition, which, in contrast to that reported for the majority of cobalt(II) SCO complexes, is strongly cooperative with a thermal hysteresis *ca.* 33 K wide. It corresponds to a "re-entrant" structural phase transition in which the IP state almost doubles the unit cell volume of the pure HS and LS phases. The lack of an inclined plateau in the warming mode indicates that the IP state is quite unstable in this mode and rapidly converts to the "normal high temperature" phase, thus defining a small-amplitude second hysteresis loop *ca.* 10–12 K wide, which resembles the behaviour reported by Hayami and co-workers for $[Co(4\text{-terpyOC}_n)_2](BF_4)_2$.

The change of the unit cell volume experienced between 293 K and 120 K for **1**, $\Delta V = V(293\text{ K}) - V(120\text{ K}) = 1786.4 - 1735.0 = 51.4$ Å^3 or 25.7 Å^3 per cobalt(II) ion ($Z = 2$), is much larger than that expected for a SCO cobalt(II) compound. ΔV contains two components: one corresponds to the volume variation due to the SCO, and the other is related to the thermal contraction/dilation, which is usually large for mononuclear compounds.[28] Interestingly, ΔV is significantly larger for **2**, $\Delta V = V(293\text{ K}) - V(120\text{ K}) = 1832.2 - 1748.4 = 83.8$ Å^3 or 41.9 Å^3 per cobalt(II) ion. Furthermore, the unit cell volume measured for **2** in the IP, 3539.92 Å^3 ($Z = 4$), represents a decrease in volume of *ca.* 31 Å^3 per cobalt(II) ion despite the increase in the HS population observed from the magnetic measurements. This value correlates well, at least qualitatively, with the decrease observed for the average Co–N bond distances in both cobalt sites in the IP and suggests that the cobalt ions are in a compressed metastable HS state. The remaining volume variation, *ca.* 11 Å^3, takes place essentially in a discontinuous step involving a complete transformation from the HS state to the LS state on cooling. Unfortunately, the quality of the X-ray data in the LS state precludes any reasonable discussion about the microscopic structural changes (*i.e.* π–π stacking, hydrogen bonds, $[CoN_6]$ environment) involved in this first order spin transition. It is important to remark that the crystal does not crack in this step since, when it is warmed at 293 K, the X-ray data are reasonably good.

In a recent paper Törnroos and co-workers have investigated the interplay of spin conversion and structural phase transformations in the 2-propanol solvate of tris(2-picolylamine)iron(II) dichloride. The crystal structure of this compound was investigated at fourteen temperatures in the cooling mode and at seven temperatures in the warming mode. This study revealed that changes in intermolecular interactions or at the immediate environment of the complex cation are related to the cooperativity of spin crossover in a complicated way that does not seem to follow simple rules.[29] This assertion may apply for the first order spin transition coupled with a crystallographic phase transition observed in polymorph **2**.

Conclusion

Here we have reported on the occurrence of polymorphism in $[Co(4\text{-terpyridone})_2](CF_3CO_3)_2{\cdot}H_2O$. Polymorph **1** undergoes a continuous spin conversion similar to that previously reported for other salts of the same cationic complex. However, polymorph **2** presents the first example of a "reverse" spin transition triggered by a crystallographic phase transition

not associated to the presence of long alkyl chains attached to the terpyridine-like ligands of the cationic cobalt(II) complex. In the new structural phase the Co(II) cations undergo strong cooperative spin transition characterised by a large hysteresis loop.

Experimental

Materials

$CoSO_4{\cdot}7H_2O$, KCF_3SO_3 and 2,6-bis(2-pyridyl)-4(1*H*)-pyridone were purchased from commercial sources and used as received.

Synthesis of 1 and 2

The synthesis of polymorphs **1** and **2** was performed under an argon atmosphere. A mixture of $CoSO_4{\cdot}7H_2O$ (0.5 mmol) and KCF_3SO_3 (1 mmol) was stirred in CH_3OH–H_2O (75 : 25, 15 mL) for 30 min. The resulting pink solution Co(II)–$2CF_3SO_3^-$ was separated from the formed K_2SO_4 and subsequently added to a methanolic solution of 4-terpyridone (1 mmol, 15 mL) under continuous stirring. The final red-brown solution was allowed to evaporate under an argon stream (5–6 days) to give rectangular brown crystals of **1**. The crystals were washed with small amounts of water and dried in an argon stream (yield: 70%). Found: C, 43.3%; H, 2.7%; N, 9.5%. $C_{32}H_{24}N_6O_9S_2F_6Co$ requires C, 43.9%; H, 2.7%; N, 9.6%. Single crystals of polymorph **2** (needles) were formed in same way; however, evaporation was carried out much faster (*ca.* 24 h). The constitutive nature of this polymorph was characterised from single crystal X-ray diffraction techniques.

X-Ray crystallographic study

Diffraction data for polymorphs **1** and **2** were collected with a Nonius Kappa-CCD single crystal diffractometer using Mo-Kα radiation (λ = 0.71073 Å). A multi-scan absorption correction was found to have no significant effect on the refinement results. The structures were solved by direct methods using SHELXS-97 and refined by full-matrix least-squares on F^2 using SHELXL-97.[30] All non-hydrogen atoms were refined anisotropically.

Magnetic susceptibility measurements

Variable-temperature magnetic susceptibility measurements were performed on single crystals of **1** and **2** (scan rate temperature equal to 2 K min^{-1}) by using a Quantum Design MPMS2 SQUID susceptometer equipped with a 5.5 T magnet and operating at 1 T and 1.8–375 K. Experimental data were corrected for constitutive diamagnetism using Pascal's constants and for magnetic contribution of the sample holder.

Acknowledgements

Financial support from the Spanish Ministerio de Educacion y Ciencia (MEC) (CTQ 2007-64727) is acknowledged. A.B.G. thanks the Spanish MEC for a research contract (Programa Ramón y Cajal). We also acknowledge the European Project MAGMANET.

References

1 *Spin Crossover in Transition Metal Compounds*, ed. P. Gütlich and H. A. Goodwin, *Top. Curr. Chem.*, 2004, vol. 233, 234, 235.
2 P. Gütlich, A. Hauser and H. Spiering, *Angew. Chem., Int. Ed. Engl.*, 1994, **33**, 2024.
3 J. A. Real, A. B. Gaspar, V. Niel and M. C. Muñoz, *Coord. Chem. Rev.*, 2003, **236**, 121.
4 J. A. Real, A. B. Gaspar and M. C. Muñoz, *Dalton Trans.*, 2005, 2062.
5 H. A. Goodwin, *Top. Curr. Chem.*, 2004, **234**, 49.
6 P. Gütlich and Y. Garcia, *Top. Curr. Chem.*, 2004, **234**, 23.
7 S. Kremer, W. Henke and D. Reinen, *Inorg. Chem.*, 1982, **21**, 3013.
8 B. N. Figgis, E. S. Kucharski and A. W. White, *Aust. J. Chem.*, 1983, **36**, 1537.
9 O. Kahn, R. Claude and H. Coudane, *Nouv. J. Chim.*, 1980, **4**, 167.
10 (*a*) J. Zarembowitch, R. Claude and O. Kahn, *Inorg. Chem.*, 1985, **24**, 1576; (*b*) J. Zarembowitch, *New J. Chem.*, 1992, **16**, 255.
11 J. Zarembowitch and O. Kahn, *Inorg. Chem.*, 1984, **23**, 589.
12 P. Thuéry and J. Zarembowitch, *Inorg. Chem.*, 1986, **25**, 2001.
13 J. Faus, M. Julve, F. Lloret, J. A. Real and J. Seletten, *Inorg. Chem.*, 1994, **33**, 5335.
14 K. Mizuno and J. H. Lunsford, *Inorg. Chem.*, 1983, **22**, 3484.
15 S. Tiwary and S. Vasudevan, *Inorg. Chem.*, 1998, **37**, 5239.
16 R. Sieber, S. Decurtins, H. Stoeckli-Evans, C. Wilson, D. Yifit, J. A. K. Howard, S. C. Capelli and A. Hauser, *Chem.–Eur. J.*, 2000, **6**, 361.
17 S. Brooker, P. G. Plieger, B. Moubaraki and K. S. Murray, *Angew. Chem., Int. Ed.*, 1999, **38**, 408.
18 S. Brooker, D. J. De Geest, R. J. Kelly, P. G. Plieger, B. Moubaraki, K. S. Murray and G. B. Jameson, *J. Chem. Soc., Dalton Trans.*, 2002, 2080.
19 R. Clérac, F. A. Cotton, L. M. Daniels, K. R. Dunbar, K. Kirschbaum, C. A. Murillo, A. A. Pinkerton, A. J. Schultz and X. Wang, *J. Am. Chem. Soc.*, 2000, **122**, 6226.
20 R. Clérac, F. A. Cotton, K. R. Dunbar, C. A. Murillo and X. Wang, *Inorg. Chem.*, 2001, **40**, 1256.
21 R. Clérac, F. A. Cotton, K. R. Dunbar, T. Lu, C. A. Murillo and X. Wang, *J. Am. Chem. Soc.*, 2000, **122**, 2272.
22 S. Hayami, K. Hashiguchi, G. Juhász, M. Ohba, H. Ohkawa, Y. Maeda, K. Kato, K. Osaka, M. Takata and K. Inoue, *Inorg. Chem.*, 2004, **43**, 4124.
23 A. B. Gaspar, M. C. Muñoz and J. A. Real, *Inorg. Chem.*, 2001, **40**, 9.
24 A. Galet, A. B. Gaspar, M. C. Muñoz and J. A. Real, *Inorg. Chem.*, 2006, **45**, 4413.
25 (*a*) S. Hayami, Y. Shigeyoshi, M. Akita, K. Inoue, K. Kato, K. Osaka, M. Takata, R. Kawajiri, T. Mitani and Y. Maeda, *Angew. Chem., Int. Ed.*, 2005, **44**, 4899; (*b*) S. Hayami, R. Moriyama, Y. Kawajiri, T. Mitani, M. Akita, K. Inuoe and Y. Maeda, *Inorg. Chem.*, 2005, **44**, 7295; (*c*) S. Hayami, R. Moriyama, A. Shuto, Y. Maeda, K. Ohta and K. Inuoe, *Inorg. Chem.*, 2007, **46**, 7692; (*d*) M. Seredyuk, A. B. Gaspar, V. Ksenofontov, Y. Galyametdinov, J. Kusz and P. Gütlich, *Adv. Funct. Mater.*, 2008, **18**, 2089.
26 R. J. Davey, *Chem. Commun.*, 2003, 1463.
27 J. D. Dunitz and J. Bernstein, *Acc. Chem. Res.*, 1995, **28**, 193.
28 J. A. Real, B. Gallois, T. Granier, F. Suez-Panama and J. Zarembowitch, *Inorg. Chem.*, 1992, **31**, 4972.
29 K. W. Törnroos, M. Hostettler, D. Chernyshov, B. Vagdal and H. B. Bürgi, *Chem.–Eur. J.*, 2006, **12**, 6207.
30 G. M. Sheldrick, *SHELX97, Program for Crystal Structure Determination*, University of Gottingen, Germany, 1997.